

Excitation of bubble surface plasmons in rare-gas-irradiated aluminum films

A. vom Felde and J. Fink

Kernforschungszentrum Karlsruhe, Institut für Nukleare Festkörperphysik,
Postfach 3640, D-7500 Karlsruhe, Federal Republic of Germany

(Received 19 February 1985)

Neon, argon, and xenon bubbles in aluminum have been investigated by means of electron-energy-loss spectroscopy. The spectra of the aluminum films containing neon or argon bubbles show the existence of bubble surface plasmons, whereas those containing xenon bubbles do not exhibit a bubble surface plasmon. A treatment by the effective-medium theory was successful in explaining positions and intensities of the bubble surface plasmons or their disappearance.

Rare gases in metals, introduced by ion implantation or nuclear processes, are essentially insoluble and tend to precipitate in bubbles.¹ The bubble and the host metal constitute an inner interface at which electron oscillations, the so-called bubble surface plasmons (BSP), can be excited. The first experimental confirmation of its existence was given by Henoc and Henry.² Recently, BSP at the inner surface of the bubbles in aluminum were investigated by Manzke and co-workers.^{3,4}

This paper deals with electron-energy-loss measurements (EELS) at rare-gas-irradiated aluminum films. BSP's were found in the spectra of Al films containing Ne or Ar bubbles. Surprisingly the spectrum of the Xe-implanted specimen lacks a BSP; it is suppressed as a consequence of coupling of the surface plasmon oscillation and the valence electron excitations in Xe. The properties of the BSP result from the dielectric functions of the host metal and of the medium in the bubbles. So, an effective-medium theory was used for understanding the features, and indeed it accounts for the energy positions and intensities of the BSP's in the case of Ne and Ar bubbles as well as for the anomalous behavior in the case of Xe bubbles.

Epitaxially grown aluminum films with a grain size of about 2000 Å and with a thickness of almost 1000 Å were produced by evaporation of Al on a NaCl(100) surface. A homogeneous distribution of the rare-gas atoms in the Al host matrix was realized by implanting at room temperature with different energies and doses. In all cases the total amount of implanted Ne, Ar, and Xe was 3 at.%. In the case of Ar and Xe, the trapped amount was determined by Rutherford backscattering measurements to be 2.0 and 2.2 at.%, respectively. Transmission-electron microscope (TEM) studies of the bubble radii were performed in a Philips EM 400 T microscope and yielded bubble radii of about 15 Å. Previous EELS experiments⁵ revealed overpressurized bubbles, containing liquid Ne and solid Ar and Xe at room temperature. In the case of Xe, epitaxial growth of the rare gas in the Al matrix was observed⁵ in EELS elastic spectra and in TEM diffraction pattern. The epitaxial growth of rare-gas bubbles in various matrices was recently confirmed in similar investigations.⁶ Transmission EELS measurements at room temperature were performed with a high-resolution 170-keV spectrometer. The energy and momentum resolution were chosen to be 0.14 eV and 0.04 Å⁻¹, respectively.

Figure 1 shows the EELS spectra of the Al/Ne, Al/Ar, and Al/Xe samples in the energy region from 0 to 20 eV. Energy-loss maxima at 6.8 and 15 eV can be ascribed to the

surface plasmon on the oxide coated Al film and to the Al volume plasmon, respectively. BSP's are located at 11.7 eV in the Al/Ne spectrum and at 10.2 eV in the Al/Ar spectrum. Arrows in Fig. 1 mark valence electron excitations ($1S_0-1P_1$) in Ar and Ne occurring at 12.8 and 18.3 eV, respectively. Note that these transitions are broadened and considerably shifted to higher energies in comparison with their atomic transition energies of 11.8 and 16.9 eV, due to the high densities and pressures of the rare gases in the bubbles of about 40 kbar.⁵ In the energy region from 7 to 11 eV, where the BSP is expected to appear, the Al/Xe spectrum exhibits a somewhat complicated structure, again marked by arrows. From EELS measurements carried out by Keil,⁷ it is known that in this energy region the lowest possible Xe valence electron excitations occur, but the observed structure in Fig. 1 is completely distinct from Keil's results.⁷

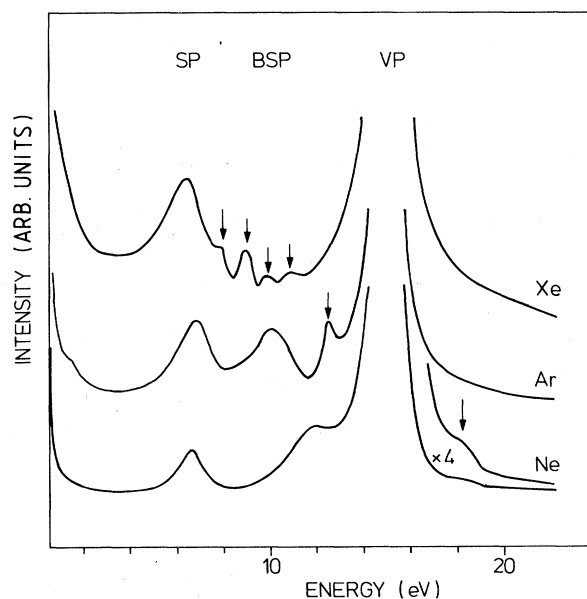


FIG. 1. Energy-loss spectra of Al films implanted with about 3 at.% Ne, Ar, and Xe, at momentum transfer $q = 0$. The Al/Ar and the Al/Xe spectra were taken on annealed samples. SP: Al surface plasmon; BSP: bubble surface plasmon; VP: Al volume plasmon. Arrows on the Al/Ne and Al/Ar curves indicate valence electron transitions of the rare-gas atoms. Arrows on the Al/Xe curve mark coupled oscillations between Xe valence electron transitions and the BSP.

The *Al*/Ar and *Al*/Xe spectra shown were taken on samples annealed in several steps up to 560°C. The reason for this is that exposing the sample to elevated temperatures causes the bubbles to grow. As a consequence the pressure in the bubbles decreases and the pressure-induced shifts of the transition energies as well as the pressure-induced broadening of the interband transitions are reduced. Thus, excitations are better resolved in the spectra. During annealing no remarkable effect on the BSP energies and intensities was found.

In Fig. 2 we present the spectra of *Al*/Xe with momentum transfer increasing from 0.0 to 0.2 Å⁻¹ in the energy region from 7 to 11 eV. Obviously a complete change of the spectrum takes place, more or less continuously proceeding with increasing momentum transfer. For $q > 0.15$ Å⁻¹ new maxima appeared at 8.4, 9.6, and 10.4 eV.

In the following we show that all these features can be explained satisfactorily by an effective-medium theory. The effective-medium theory, advanced by Garnett,⁸ describes the long-wavelength dielectric properties of a composite medium. From the dielectric function $\epsilon_I, \epsilon_{II}$ of the host medium I and the dispersed medium II, respectively, an effective dielectric function is constructed via the relation

$$\frac{\epsilon_{\text{eff}} - \epsilon_I}{\epsilon_{\text{eff}} + 2\epsilon_I} = f \frac{\epsilon_{II} - \epsilon_I}{\epsilon_{II} + 2\epsilon_I}$$

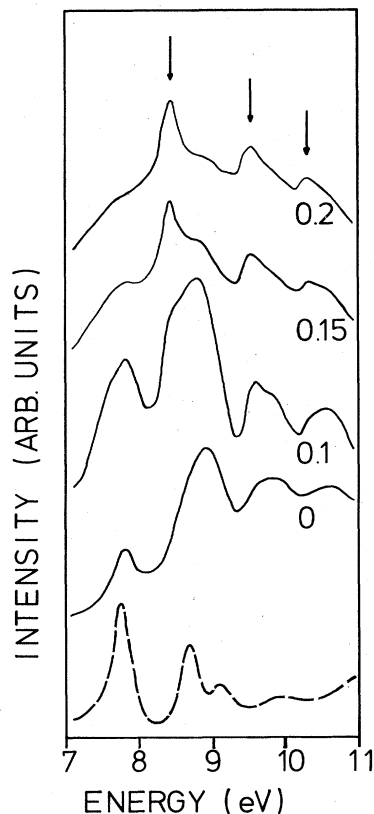


FIG. 2. Energy-loss spectra of the *Al*/Xe sample, taken with momentum transfers $q = 0.0, 0.1, 0.15,$ and 0.2 Å⁻¹. Arrows on the uppermost curve mark Xe valence electron transitions. The intensity due to the SP losses was subtracted from the spectra. The dashed curve shows the energy-loss function calculated on the basis of Garnett theory.

f is the so-called filling factor, i.e., the volume fraction of the medium II. We apply this theory to our case of rare-gas bubbles dispersed in an aluminum host matrix. It should be noted that the Maxwell-Garnett theory⁸ is based on the Clausius-Mosotti equation which requires that the bubbles form a cubic lattice. Persson and Liebsch⁹ extended these calculations to a random distribution of bubbles in the host material resulting in a slight red shift and a considerable broadening of the BSP spectral function.

The dielectric function of Al can be described by a Drude model. Ne, Ar, and Xe dielectric functions were satisfactorily reproduced by means of several oscillators with Lorentzian shape. The filling factors were calculated from measurements of the rare-gas content by Rutherford back-scattering experiments and from mean values of the rare-gas densities and the bubble radii given in Ref. 5. In the case of *Al*/Xe, where we discuss the spectra taken on annealed samples, the filling factor is comparably higher and was estimated to be about 8%.

Finally, the electron energy losses, which are proportional to the energy-loss function $\text{Im}(-1/\epsilon)$, were calculated from the effective dielectric function ϵ_{eff} . Figure 3 presents the calculated energy-loss spectra. The theoretically calculated BSP energies for *Al*/Ar and *Al*/Ne were 10.0 and 11.4 eV, respectively, whereas 10.2 and 11.7 eV were measured. These small deviations may be due to inaccuracies in the values for the electron density used in the Lorentz model. Calculated intensities—all normalized to the Al volume plasmon intensity—are 0.064 and 0.018 for *Al*/Ne and *Al*/Ar, respectively, whereas about 0.05 and 0.022 were measured. So, BSP energies and intensities are well reproduced within the simple effective-medium theory. The theory also provides the energy losses due to the rare-gas excitations in Ne and Ar and due to the Al volume plasmon. The observed half-widths of the BSP's considerably exceed the calculated ones. Our calculations show that the half-width of the BSP is nearly insensitive to any reasonable variation of the parameters used in the Lorentz model. As already mentioned above, the discrepancies can be explained by a random distribution of rare-gas bubbles.⁹ As can be seen in

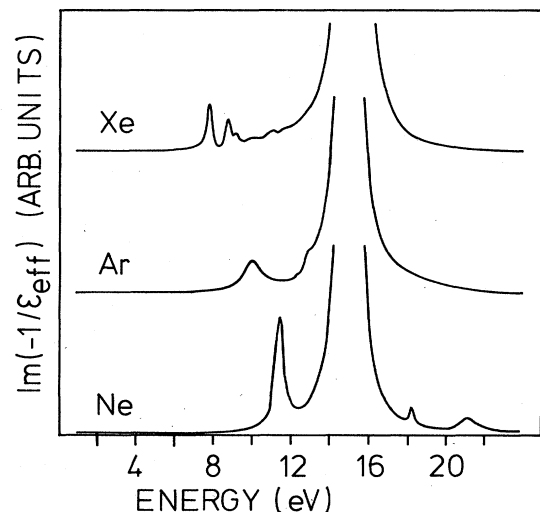


FIG. 3. Energy-loss functions calculated with the effective-medium theory for *Al*/Ne ($f = 3\%$), *Al*/Ar ($f = 3\%$), and *Al*/Xe ($f = 8\%$).

Fig. 3, the theory also accounts for the absence of a BSP in the case of Al/Xe. Moreover, the structure of the measured Al/Xe spectrum from 7 to 11 eV for $q=0$ (Fig. 1 and Fig. 2, $q=0$) can be explained by the calculations in the framework of effective-medium theory (see Fig. 2, dashed curve). Maxima occurring slightly beyond 8, 9, 10, and 11 eV in the measured spectrum correspond to those calculated, disregarding the comparably low intensity of the first peak and the fact that in the measured spectrum the two oscillators near 9 eV are not resolved. Moreover, the fourth maximum has a slightly higher energy in the calculated spectrum. The discrepancies can be explained by not exact values for the damping of the Xe oscillators and by the fact that all interband transitions beyond 12 eV were approximated by one oscillator having a high oscillator strength. The calculated energy-loss functions do not reproduce the Al surface plasmon, because the effective-medium theory does not consider outer surfaces.

In Fig. 4 we illustrate the influence of the filling factor on the BSP. Curves (a) and (b) show $\epsilon_{\text{eff}1}$ and $\text{Im}(-1/\epsilon_{\text{eff}})$ for the filling factor $f=8\%$, curves (c) and (d) for $f=50\%$. For low filling factors $f < 10\%$, the real as well as the imaginary part of the dielectric function of Al are only slightly disturbed by the presence of Xe bubbles. The influence increases with increasing filling factor and an additional zero intersection of $\epsilon_{\text{eff}1}$ may be produced, as shown in curve (c). This zero intersection [see curve (d)] causes a strong maximum in the energy-loss function, which we suppose to be the BSP. From this, it can be seen that the lower the energy of the valence electron excitations, the higher the filling factor has to be in order to observe a BSP. To proof this prediction, Al samples were implanted with higher Xe doses in order to increase the filling factor. Unfortunately, higher

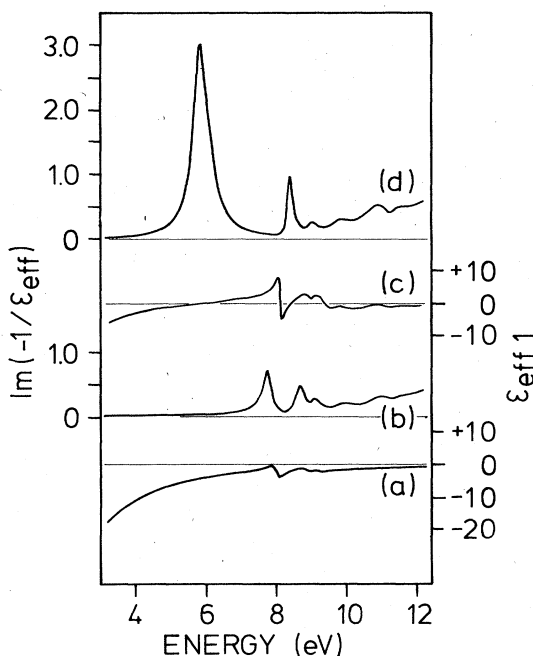


FIG. 4. Real part $\epsilon_{\text{eff}1}$ and energy-loss function $\text{Im}(-1/\epsilon_{\text{eff}})$ of the effective dielectric function of Al/Xe. (a) $\epsilon_{\text{eff}1}$ for $f=8\%$; (b) $\text{Im}(-1/\epsilon_{\text{eff}})$ for $f=8\%$; (c) $\epsilon_{\text{eff}1}$ for 50%; (d): $\text{Im}(-1/\epsilon_{\text{eff}})$ for 50%.

implantation doses destroyed the Al films. Another proof which has not yet been carried out is the implantation of Kr in Al. Valence electron excitations of Kr have slightly higher transition energies than those of Xe. Hence, following the model outlined above, a BSP should be observed at even lower filling factors. Suppose the model applies well, it seems to be possible to produce Kr bubbles in Al exhibiting or lacking a BSP in EELS experiments according to how the implantation conditions (and thus the filling factor) were chosen.

Let us return to the case of Al/Xe, where the coupling of BSP and Xe valence electron excitations lead to a damping of the BSP and to a complete distortion of the spectrum of Xe valence electron transitions. This interpretation is corroborated by the observed momentum dependence of these excitations (Fig. 2). EELS measurements at zero scattering angle (i.e., $q=0$, $\Delta q < 0.04 \text{ \AA}^{-1}$) provide information on electronic excitations without resolving the spatial peculiarities. The collective electron oscillations have a long wavelength; i.e., electrons oscillate in phase over extended regions compared with bubble sizes. The electronic properties detected in such an experiment are characteristic for a medium having an effective dielectric function ϵ_{eff} , based on the dielectric functions of its components. Hence, EELS measurements taken at $q=0$ are adequately described by the Maxwell-Garnett theory.

Spatial variations in electronic structure and thus decoupling can only be observed in EELS spectra taken at nonzero momentum transfer. Decoupling of volume plasmons in Al-Mg alloys was observed in EELS spectra taken at sufficiently high momentum transfer so that the plasmon wavelength was smaller than the size of the Al or Mg grains, respectively.¹⁰ This effect may be due to localization of the plasmon oscillation with increasing momentum transfer q . However, the effect of increased damping with increasing momentum transfer q is not very pronounced. In the case of surface plasmons it is well known that the plasma oscillation becomes strongly concentrated near the boundary with increasing wave vector. Its electronic field E decays in a direction (z) normal to the boundary as $E \sim \exp(-qz)$ (q is the wave vector of the surface plasmons).¹¹ Hence, coupling of BSP with Xe valence electron excitations should vanish with increasing wave vector. Moreover, the excitation probability of a BSP vanishes rapidly with increasing momentum transfer q . From EELS measurements it is known that at $q=0.15 \text{ \AA}^{-1}$ the BSP is almost quenched and so the less q dependent Xe valence electron transitions should remain undisturbed at $q \geq 0.15 \text{ \AA}^{-1}$. Indeed, the EELS spectra on Al/Xe at $q=0.15$ and 0.2 \AA^{-1} (Fig. 2, arrows) reveal the expected Xe valence electron excitations, observed by Keil⁷ at 8.41, 9.51, and 10.37 eV.

In these considerations no pressure-induced energy shifts are involved. First, the Al/Xe spectra used were taken on annealed samples containing large bubbles. These shifts result from the overlap of the atomic wave functions of the excited rare-gas atoms with wave functions of the neighboring rare-gas atoms. Thus, the shift decreases when the rare-gas density and pressure is reduced by bubble growth. Second, the relative spatial extension of the excited p wave function decreases in going from He to Xe. Hence, the overlap of the p and s wave functions of neighboring atoms in the ground state decreases as the atomic number is increased. Similar measurements on nonannealed samples

yielded no information since due to the pressure-induced broadening, excitations were not resolvable.

In summary, the effective-medium theory is a simple but useful concept in clarifying plasmon losses in composite media. In the case of electronic excitation energies near the expected BSP energy, damping of the BSP and complete distortion of the spectrum of the electronic excitations arises. For a detailed understanding of the observed momentum

dependence of the energy-loss spectra, an effective-medium theory which accounts for frequency- and momentum-dependent dielectric functions is required.

We are indebted to R. von Baltz and H. Rietschel for many helpful discussions. The authors are also grateful to G. Linker and B. Scheerer for sample preparation and to D. Kaletta for his transmission-electron-microscopy studies.

-
- ¹J. von den Driesch and P. Jung, *High Temp. High Pressures*, **12**, 635 (1980).
²P. Henoc and L. Henry, *J. Phys. (Paris) Colloq.* **31**, Suppl. 4, C1-55 (1970).
³R. Manzke and M. Campagna, *Solid State Commun.* **39**, 313 (1981).
⁴R. Manzke, G. Crecelius, and J. Fink, *Phys. Rev. Lett.* **51**, 1095 (1983).
⁵A. vom Felde, J. Fink, Th. Müller-Heinzerling, J. Pflüger, B. Scheerer, G. Linker, and D. Kaletta, *Phys. Rev. Lett.* **53**, 922 (1984).
⁶C. Templier, C. Jaouen, J.-P. Rivière, J. Delafond, and J. Grilhe, *C. R. Acad. Sci.* **299**, 613 (1984); J. H. Evans and D. J. Mazey, *J. Phys. F* **15**, L1 (1984).
⁷P. Keil, *Z. Naturforsch. Teil A* **21**, 503 (1966).
⁸J. C. Maxwell Garnett, *Philos. Trans. R. Soc. London* **203**, 385 (1904); **205**, 237 (1906).
⁹B. N. J. Persson and A. Liebsch, *Solid State Commun.* **44**, 1637 (1982).
¹⁰H. Möller and A. Otto, *Solid State Commun.* **38**, 977 (1981).
¹¹H. Raether, in *Excitations of Plasmons and Interband Transitions by Electrons*, edited by G. Höhler and E. A. Niekisch, Springer Tracts in Modern Physics, Vol. 88 (Springer, New York, 1980), p. 121.